Journal of Sound and Vibration (2001) **246**(2), 337–348
doi:10.1006/jsvi.2001.3652, available online at http://www.idealibrary.com on IDEAL®

TIME–HARMONIC ELASTODYNAMIC GREEN FUNCTIONS OF PLATES FOR LINE LOADS

L. SUN

Department of Civil Engineering, ECJ Hall 6.10, The University of Texas at Austin, Austin, TX 78712, U.S.A. E-mail: lusun@mail.utexas.edu

(*Received* 15 *September* 2000, *and in final form* 12 *February* 2001)

In this paper the Fourier transform is used to derive the elastodynamic Green function of a plate on a viscoelastic foundation subjected to impulse and harmonic line loads. The solution is first given as a convolution of the Green function of the plate. Poles of the integrand in the integral representation of the solution are identified for different cases of damping and load frequency. The Green function corresponding to an impulse line load is obtained and can be numerically computed. The theorem of residue is then utilized to evaluate the generalized integral of the Green function corresponding to a harmonic line load. This representation permits one to construct algorithms for the parameter identification of the inverse problem involved in a pavement non-destructive test. Validation of the result is partly verified by comparing the static solution of a point source obtained from this paper to a well-known result.

1. INTRODUCTION

Non-destructive testing (NDT) and evaluation have received much attention in the field of pavement engineering since the 1980s (see references [1–4]). As two of the most commonly used non-destructive testing devices for pavement structural evaluation, both falling weight deflectometer (FWD) and Dynaflect apply dynamic loads on the pavement surface. The primary difference between the loads applied by the FWD and the Dynaflect is that the former is an impact load, while the latter is a steady state load, i.e., a vibratory load (see reference [2]). The structural evaluation is achieved based on the response of the pavement structure to the dynamic load.

Given the complexity of the inverse problems, currently, a widely used technique for the parameter estimation of pavement structures involves the use of the forward static analysis of the pavement structure, and then a comparison of the measured response with the calculated response. Usually, the physical model for simplifying rigid pavements (cement concrete pavements) is a plate on either an elastic Winkler foundation or an elastic half-space (see reference [5]). Parameters of pavements are eventually determined by selecting the parameters of a pavement structure whose calculated response is closest to the measured response in terms of certain objective functions (see reference [6]). Clearly, since the calculated response of the pavement is based on the static analysis, which ignores the time, inertial and damping effects, the theoretical model is apparently inconsistent with the realistic loading condition (see reference [3]).

To better understand the dynamic response of pavement structures to the FWD and Dynaflect loading, it is indispensable to analyze the fundamental response of pavement

0022-460X/01/370337 + 12 $35.00/0

structures under impact and vibrating loads. Several finite-element procedures have been developed to carry out the response of a thin plate to dynamic loads (see references [7–9]). Regarding the analytical solution, the response of an infinite plate on an elastic foundation to harmonic plane waves has been investigated for many years. Deshun [10] applies the variational principle to solve the vibration of thick plates. The vertical vibration of an elastic plate on a fluid-saturated porous half-space subjected to a harmonic load is investigated by Bo [11], in which the Hankel transform is used to convert the governing equation to a Fredholm integral equation of the second order and numerical calculation can then be carried out.

Another motivation for studying this problem is the fact that the fundamental solution of plate plays an important role when the boundary element method (BEM) is applied to treat the dynamic problem of a plate resting on an elastic foundation. It has been demonstrated that pavement loading is a random process (see reference [12]). The boundary integral equation suitable to analyze the static response of a plate on an elastic foundation is derived based on the analytical representation of the static fundamental solution of a thin plate. The availability of the dynamic fundamental solution of a thin plate is theoretically of value for applying the BEM to the dynamic analysis of a thin plate.

This paper studies the analytical solutions of a thin plate (i.e., the rigid pavement model) on a viscoelastic foundation subjected to an impulsive line load and a harmonic line load. The impulse response of the plate serves as a fundamental solution for constructing the dynamic response of a plate to the FWD load in the time domain, and the harmonic response of the plate serves as a fundamental solution for constructing the dynamic response of the plate to the Dynaflect load in the frequency domain.

2. THE GOVERNING EQUATION

Figure 1 depicts the co-ordinate system and significant dimensions. The infinite length of the plate runs along the x- and y-axis respectively. Three assumptions are made to simplify the mathematical model of a thin plate. These assumptions are: (1) the strain component ε_z in the perpendicular direction of the plate is sufficiently small to be ignored; (2) the stress components τ_{zx}, τ_{zy}, and σ_z are far less than the other stress components; therefore, the deformation caused by τ_{zx}, τ_{zy}, and σ_z is negligible; and (3) the displacement parallel to the horizontal direction of the plate is zero.

Denote the displacement of the plate in the z direction as $W(x, y, t)$. Based on these assumptions and the fundamental equations of elastodynamics, the governing equation for

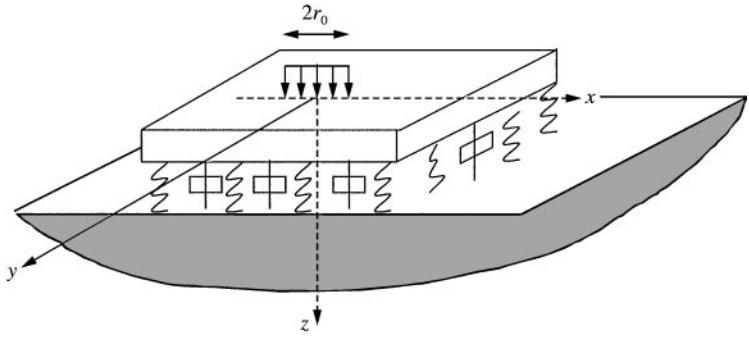

Figure 1. A thin plate resting on a viscoelastic foundation.

the deflection of the plate can be derived by considering the balance of all the forces acting on the element $(x, x + \mathrm{d}x;\ y, y + \mathrm{d}y)$. Those forces are the impressed force distribution $F(x, y, t)$, the shearing force, the restoring force from the foundation $q(x, y, t)$, and the inertial force $\rho h \partial^2 W/\partial t^2$. The well-known result is (see references [13, 14])

$$D\nabla^2\nabla^2 W(x, y, t) + \rho h \frac{\partial^2}{\partial t^2} W(x, y, t) = F(x, y, t) - q(x, y, t), \tag{1}$$

where the Laplace operator $\nabla^2 = \partial^2/\partial x^2 + \partial^2/\partial y^2$. Also, the so-called stiffness of plate $D = Eh^3/[12(1 - \mu^2)]$, h is the thickness of plate, ρ is the density of plate medium, and E and μ are Young's modulus of elasticity and the Poisson ratio of the elastic plate respectively.

As one of the most commonly used foundation models in rigid pavement design (i.e., cement concrete pavements), the Winkler elastic foundation model performs well in many circumstances (see references [13–16]). The Winkler foundation model assumes that the reactive pressure is proportional to the deflection of the plate, that is $q = KW$. The term K is called the modulus of subgrade reaction. The assumption that K is constant implies linear elasticity for the subgrade. In reality, damping effects appear in any dynamic system. If the damping effect of the subgrade is considered, the restoring force $q = KW + C\partial W/\partial t$. This is a viscoelastic foundation model consisting of a spring of strength K and a dashpot of strength, C, placed parallel. Substitution of the restoring force into equation (1) gives

$$D\nabla^2\nabla^2 W(x, y, t) + KW(x, y, t) + C\frac{\partial}{\partial t} W(x, y, t) + \rho h \frac{\partial^2}{\partial t^2} W(x, y, t) = F(x, y, t). \tag{2}$$

3. THE GREEN FUNCTION

According to the theory of mathematical–physical equation, the Green function of a partial differential equation represents the fundamental solution of the equation as the load condition is in the form of the Dirac-delta function (see references [13, 17]). For the current problem, the Green function of the plate is defined as the solution of equation (2), given that the external excitation $F(x, y, t)$ is characterized by

$$F(\mathbf{x}) = \boldsymbol{\delta}(\mathbf{x} - \mathbf{x}_0), \tag{3}$$

in which $\mathbf{x} = (x, y, t)$, $\mathbf{x}_0 = (x_0, y_0, t_0)$, $\boldsymbol{\delta}(\mathbf{x} - \mathbf{x}_0) = \delta(x - x_0)\delta(y - y_0)\delta(t - t_0)$, and $\delta(\cdot)$ is the Dirac-delta function. It is defined by

$$\int_{-\infty}^{\infty} \delta(x - x_0) f(x)\,\mathrm{d}x = f(x_0). \tag{4}$$

Define the three-dimensional Fourier transform and its inversion as

$$\tilde{f}(\boldsymbol{\xi}) = \mathbf{F}[f(\mathbf{x})] = \int_{-\infty}^{\infty}\int_{-\infty}^{\infty}\int_{-\infty}^{\infty} f(\mathbf{x}) \exp(-\mathrm{i}\boldsymbol{\xi}\mathbf{x})\,\mathrm{d}\mathbf{x}, \tag{5a}$$

$$f(\mathbf{x}) = \mathbf{F}^{-1}[\tilde{f}(\boldsymbol{\xi})] = (2\pi)^{-3}\int_{-\infty}^{\infty}\int_{-\infty}^{\infty}\int_{-\infty}^{\infty} \tilde{f}(\boldsymbol{\xi}) \exp(\mathrm{i}\boldsymbol{\xi}\mathbf{x})\,\mathrm{d}\boldsymbol{\xi}, \tag{5b}$$

where $\boldsymbol{\xi} = (\xi, \eta, \omega)$, $\mathbf{F}[\cdot]$ and $\mathbf{F}^{-1}[\cdot]$ are the Fourier transform and its inversion respectively. To solve the Green function, take the three-dimensional Fourier transform of both sides of equation (2):

$$D(\xi^2 + \eta^2)^2 \tilde{G}(\boldsymbol{\xi}; \mathbf{x}_0) + K\tilde{G}(\boldsymbol{\xi}; \mathbf{x}_0) + \mathrm{i}C\omega\tilde{G}(\boldsymbol{\xi}; \mathbf{x}_0) - \rho h\omega^2 \tilde{G}(\boldsymbol{\xi}; \mathbf{x}_0) = \tilde{F}(\boldsymbol{\xi}), \tag{6}$$

in which $\tilde{F}(\boldsymbol{\xi})$ is the Fourier transform of $F(\mathbf{x})$, and the displacement response $W(\mathbf{x})$ has been replaced by the symbol $G(\mathbf{x}; \mathbf{x}_0)$ to indicate the Green function, in which $\mathbf{x}$ represents the spatial position where the response of interest is located and $\mathbf{x}_0$ represents the source position where the load is applied. Also, the following property of Fourier transform is used in the derivation of equation (6):

$$\mathbf{F}[f^{(n)}(t)] = (\mathrm{i}\omega)^n \mathbf{F}[f(t)]. \tag{7}$$

Since $\tilde{F}(\boldsymbol{\xi})$ is the representation of $F(\mathbf{x})$ in the frequency domain, we also need to evaluate $\tilde{F}(\boldsymbol{\xi})$. This can be implemented by taking the three-dimensional Fourier transform of both sides of equation (3),

$$\tilde{F}(\boldsymbol{\xi}) = \int_{-\infty}^{\infty}\int_{-\infty}^{\infty}\int_{-\infty}^{\infty} \delta(\mathbf{x} - \mathbf{x}_0)\exp(-\mathrm{i}\boldsymbol{\xi}\mathbf{x})\,\mathrm{d}\mathbf{x} = \exp(-\mathrm{i}\boldsymbol{\xi}\mathbf{x}_0), \tag{8}$$

in which the property of the Dirac-delta function, i.e., equation (4), is utilized for evaluating the above integral. Substituting equation (8) into equation (6) and realizing that equation (6) is an algebraic equation, we obtain

$$\tilde{G}(\boldsymbol{\xi}; \mathbf{x}_0) = \exp(-\mathrm{i}\boldsymbol{\xi}\mathbf{x}_0)[D(\xi^2 + \eta^2)^2 + K + \mathrm{i}C\omega - \rho h\omega^2]^{-1}. \tag{9}$$

The Green function given by equation (9) is in the frequency domain and we need to convert it into the time domain. To achieve this, we take the inverse Fourier transform of equation (9) and obtain

$$G(\mathbf{x}; \mathbf{x}_0) = (2\pi)^{-3}\int_{-\infty}^{\infty}\int_{-\infty}^{\infty}\int_{-\infty}^{\infty} \exp[\mathrm{i}\boldsymbol{\xi}(\mathbf{x} - \mathbf{x}_0)][D(\xi^2 + \eta^2)^2 + K + \mathrm{i}C\omega - \rho h\omega^2]^{-1}\,\mathrm{d}\boldsymbol{\xi}. \tag{10}$$

Formula (10) is the Green function of the plate on a viscoelastic foundation. The Green function serves as a fundamental solution of a partial differential equation. It can be very useful when dealing with linear systems.

4. THE IMPULSE RESPONSE FUNCTION

The impulse response function (IRF) of the plate plays an important role when constructing solutions corresponding to non-concentrated loads. We define the IRF as the solution of equation (2) given that the term on the right-hand side of equation (2) takes the form

$$F_{IRF}(\mathbf{x}) = (2r_0)^{-1}\delta(y)\delta(t)[\mathrm{H}(x + r_0) - \mathrm{H}(x - r_0)], \tag{11}$$

where r_0 is the half-length of the line load and $\mathrm{H}(x)$ is the Heaviside function, defined as $\mathrm{H}(x) = 1$ for $x > 0$, $\mathrm{H}(x) = 0$ for $x < 0$, and $\mathrm{H}(x) = \frac{1}{2}$ for $x = 0$. According to the theory of linear partial differential equation, the solution of equation (2) given that $F(\mathbf{x})$ is taking the form of formula (11) can be constituted by integrating the Green function in all dimensions, i.e.,

$$W(\mathbf{x}) = \int_{-\infty}^{\infty} \int_{-\infty}^{\infty} \int_{-\infty}^{\infty} F(\mathbf{x}_0) G(\mathbf{x}; \mathbf{x}_0)\, \mathrm{d}\mathbf{x}_0. \tag{12}$$

Denote the IRF as $h_{Line}(\mathbf{x})$ and replace the symbol of displacement $W(\mathbf{x})$ in equation (2) by $h_{Line}(\mathbf{x})$. Substituting equations (10) and (11) into equation (12) and applying property (4) of the Dirac-delta function twice, we see that

$$h_{Line}(\mathbf{x}) = \frac{1}{(2\pi)^3} \int_{-\infty}^{\infty} \int_{-\infty}^{\infty} \int_{-\infty}^{\infty} \frac{\mathrm{H}(r_0^2 - x_0^2)\exp(\mathrm{i}\boldsymbol{\xi}\mathbf{x})\exp(-\mathrm{i}\xi x)}{2r_0[D(\xi^2 + \eta^2)^2 + K + \mathrm{i}C\omega - \rho h\omega^2]}\, \mathrm{d}\boldsymbol{\xi}\, \mathrm{d}x_0. \tag{13}$$

To evaluate this generalized integration, note that

$$\int_{-\infty}^{\infty} \frac{\mathrm{H}(r_0^2 - x_0^2)\exp(-\mathrm{i}\xi x)}{2r_0}\, \mathrm{d}x_0 = \int_{-r_0}^{r_0} \frac{\exp(-\mathrm{i}\xi x)}{2r_0}\, \mathrm{d}x_0 = \frac{\sin \xi r_0}{\xi r_0}, \tag{14}$$

in which the Euler formula

$$\exp(\mathrm{i}\varsigma) = \cos \varsigma + \mathrm{i} \sin \varsigma \tag{15}$$

is used. Compare equations (13) and (14), we can rewrite equation (13) in a more concise form,

$$h_{Line}(\mathbf{x}) = \frac{1}{(2\pi)^3} \int_{-\infty}^{\infty} \int_{-\infty}^{\infty} \int_{-\infty}^{\infty} \frac{\sin \xi r_0 \exp(\mathrm{i}\boldsymbol{\xi}\mathbf{x})}{\xi r_0[D(\xi^2 + \eta^2)^2 + K + \mathrm{i}C\omega - \rho h\omega^2]}\, \mathrm{d}\boldsymbol{\xi}. \tag{16}$$

Formula (16) is the IRF of the plate corresponding to a line load of the form of equation (11). For the IRF corresponding to a point load $F_{Point}(\mathbf{x}) = \delta(x)\delta(y)\delta(t)$, it can be simply obtained by taking limit on both sides of equation (16), i.e.,

$$h_{Point}(\mathbf{x}) = \frac{1}{(2\pi)^3} \int_{-\infty}^{\infty} \int_{-\infty}^{\infty} \int_{-\infty}^{\infty} \frac{\exp(\mathrm{i}\boldsymbol{\xi}\mathbf{x})}{D(\xi^2 + \eta^2)^2 + K + \mathrm{i}C\omega - \rho h\omega^2}\, \mathrm{d}\boldsymbol{\xi}. \tag{17}$$

Here, the following limit is used in the derivation:

$$\lim_{r_0 \to 0} \frac{\sin \xi r_0}{\xi r_0} = 1. \tag{18}$$

5. THE FREQUENCY RESPONSE FUNCTION

In this section, we use the Green function obtained in the previous section to construct the frequency response function (FRF) of the plate (i.e., the time–harmonic Green function of line loads). Denote by $W(\mathbf{x})$ the solution of equation (2) given that the external load is

a harmonic line load with the center located at the origin of the co-ordinate system, i.e.,

$$F_{FRF}(\mathbf{x}) = (2r_0)^{-1}\,\mathrm{H}(r_0^2 - x_0^2)\delta(y)\exp(\mathrm{i}\Omega t), \tag{19}$$

in which Ω is the frequency of the harmonic load. The solution of equation (2) with the right-hand-side term of this type, i.e., equation (19), becomes a steady state solution, which can be expressed as

$$W(\mathbf{x}) = \mathrm{H}_{Line}(\mathbf{x}, \Omega)\exp(\mathrm{i}\Omega t). \tag{20}$$

Here, $\mathrm{H}_{Line}(\mathbf{x}, \Omega)$ is denoted as the FRF of the plate. Expression (20) simply means that, although the response of the plate may have a phase difference with the external excitation, which is reflected in the FRF, both the response and excitation have an identical frequency Ω.

Substituting equations (19) and (20) into equation (12) and applying property (4) of the Dirac-delta function twice, we see that

$$W(\mathbf{x}) = \int_{-\infty}^{t}\int_{-\infty}^{\infty}\int_{-\infty}^{\infty}\int_{-\infty}^{\infty} \frac{\sin\xi r_0\exp(\mathrm{i}\boldsymbol{\xi}\mathbf{x})\exp[\mathrm{i}(\Omega-\omega)t_0]}{\xi r_0[D(\xi^2+\eta^2)^2 + K + \mathrm{i}C\omega - \rho h\omega^2]}\,\mathrm{d}\boldsymbol{\xi}\,\mathrm{d}t_0. \tag{21}$$

Notice the equality of integration

$$\int_{-\infty}^{\infty}\exp[\mathrm{i}(\Omega-\omega)t_0]\,\mathrm{d}t_0 = 2\pi\delta(\Omega-\omega). \tag{22}$$

Substituting equation (22) and reapplying equation (4) to formula (21) gives

$$W(\mathbf{x}) = \frac{1}{(2\pi)^2}\int_{-\infty}^{\infty}\int_{-\infty}^{\infty} \frac{\sin\xi r_0\exp(\mathrm{i}\omega t)\exp(\mathrm{i}\boldsymbol{\xi}\mathbf{x})}{\xi r_0[D(\xi^2+\eta^2)^2 + K + \mathrm{i}C\Omega - \rho h\Omega^2]}\,\mathrm{d}\xi\,\mathrm{d}\eta. \tag{23}$$

By comparing equation (23) with equation (20) it is straightforward to find

$$\mathrm{H}_{Line}(\mathbf{x}, \Omega) = \frac{1}{(2\pi)^2}\int_{-\infty}^{\infty}\int_{-\infty}^{\infty} \frac{\sin\xi r_0\exp(\mathrm{i}\boldsymbol{\xi}\mathbf{x})}{\xi r_0[D(\xi^2+\eta^2)^2 + K + \mathrm{i}C\Omega - \rho h\Omega^2]}\,\mathrm{d}\xi\,\mathrm{d}\eta. \tag{24}$$

Similar to the case of the IRF corresponding to a point load, the RFR $\mathrm{H}_{Con}(\mathbf{x}, \Omega)$ corresponding to a concentrated harmonic load $F_{Con}(\mathbf{x}) = \delta(x)\delta(y)\exp(\mathrm{i}\Omega t)$ can also be obtained by taking limit $r_0 \to 0$ on both sides of equation (24), i.e.,

$$\mathrm{H}_{Con}(\mathbf{x}, \Omega) = \frac{1}{(2\pi)^2}\int_{-\infty}^{\infty}\int_{-\infty}^{\infty} \frac{\exp(\mathrm{i}\boldsymbol{\xi}\mathbf{x})}{D(\xi^2+\eta^2)^2 + K + \mathrm{i}C\Omega - \rho h\Omega^2]}\,\mathrm{d}\xi\,\mathrm{d}\eta. \tag{25}$$

As formula (25) contains a double generalized integral, it is time consuming to evaluate equation (25) if the numerical computation is carried out. Indeed, the FRF given by equation (25) can be further simplified to a single generalized integral.

Define co-ordinate transformations

$$x = r\cos\theta, \qquad y = r\sin\theta, \qquad \xi = \zeta\cos\psi, \qquad \eta = \zeta\sin\psi. \tag{26}$$

Substitute equations (26) into equation (25) and reorganize the terms:

$$\mathrm{H}_{Con}(r, \Omega) = \frac{1}{(2\pi)^2} \int_0^{\infty} \int_0^{2\pi} \frac{\exp\{\mathrm{i}[r\zeta \sin(\theta + \psi)]\}}{D\zeta^4 + K + \mathrm{i}C\Omega - \rho h\Omega^2} \zeta \, \mathrm{d}\zeta \, \mathrm{d}\psi. \tag{27}$$

Here, the following equality is used:

$$\sin\theta \cos\psi + \cos\theta \sin\psi = \sin(\theta + \psi). \tag{28}$$

Applying Euler formula (15) to equation (27) we obtain

$$\mathrm{H}_{Con}(r, \Omega) = \frac{1}{(2\pi)^2} \int_0^{\infty} \int_0^{2\pi} \frac{\cos[r\zeta \sin(\theta + \psi)]}{D\zeta^4 + K + \mathrm{i}C\Omega - \rho h\Omega^2} \zeta \, \mathrm{d}\zeta \, \mathrm{d}\psi. \tag{29}$$

From the theory of special function we know that the Bessel function can also be expressed in terms of integration (see reference [18]).

$$\mathrm{J}_0(z) = (2\pi)^{-1} \int_0^{2\pi} \cos(z \cos\phi) \, \mathrm{d}\phi, \tag{30}$$

in which $\mathrm{J}_0(\cdot)$ is the zeroth order Bessel function of the first kind. Substituting equation (30) into equation (29) gives the final result of the FRF:

$$\mathrm{H}_{Con}(r, \Omega) = \frac{1}{2\pi} \int_0^{\infty} \frac{\mathrm{J}_0(r\zeta)}{D\zeta^4 + K + \mathrm{i}C\Omega - \rho h\Omega^2} \zeta \, \mathrm{d}\zeta. \tag{31}$$

Moreover, if the same co-ordinate transformation (26) is employed to simplify equation (17), the IRF $h_{Point}(\mathbf{x})$ can be further expressed in a more concise form as

$$h_{Point}(r, t) = \frac{1}{(2\pi)^2} \int_{-\infty}^{\infty} \int_0^{\infty} \frac{\mathrm{J}_0(r\zeta)\exp(\mathrm{i}\Omega t)}{D\zeta^4 + K + \mathrm{i}C\Omega - \rho h\Omega^2} \zeta \, \mathrm{d}\zeta \, \mathrm{d}\Omega. \tag{32}$$

So far we have obtained the FRFs $\mathrm{H}_{Line}(\mathbf{x}, \Omega)$ and $\mathrm{H}_{Con}(r, \Omega)$ in the rectangular and cylindrical co-ordinate system respectively. By comparison of equations (16) and (24), it is clear that, on the one hand, the FRF is the Fourier transform of the IRF, while on the other hand, $h_{Line}(\mathbf{x}) = (2\pi)^{-1} \int_{-\infty}^{\infty} \mathrm{H}_{Line}(\mathbf{x}, \Omega) \exp(\mathrm{i}\Omega t) \, \mathrm{d}\Omega$. In general, the FRFs given by equations (24) and (31) are complex functions and can only be calculated numerically. However, in some special cases the FRF can be analytically evaluated.

6. SPECIAL CASES

6.1. STATIC SOLUTION

It is of interest to examine the static solution by applying results (24) and (31). If the static solution obtained here is the same as the static solution obtained using other procedures, the correctness and validity of this paper can be verified to some degree.

For a static load, we have $F_{Line\_sta}(\mathbf{x}) = (2r_0)^{-1}H(r_0^2 - x^2)\delta(y)$ and $F_{Con\_sta}(\mathbf{x}) = \delta(x)\delta(y)$. The static solution of equation (2) corresponding to the static load can be achieved by letting $\Omega = 0$ in equations (24) and (31):

$$\mathrm{H}_{Line\_sta}(\mathbf{x}) = \frac{1}{(2\pi)^2}\int_{-\infty}^{\infty}\int_{-\infty}^{\infty}\frac{\sin\xi r_0\exp(\mathrm{i}\boldsymbol{\xi}\mathbf{x})}{\xi r_0[D(\xi^2+\eta^2)^2+K]}\,\mathrm{d}\xi\,\mathrm{d}\eta, \tag{33a}$$

$$\mathrm{H}_{Con\_sta}(r) = \frac{1}{2\pi}\int_0^{\infty}\frac{\mathrm{J}_0(r\zeta)}{D\zeta^4+K}\,\zeta\,\mathrm{d}\zeta. \tag{33b}$$

Expression (33b) is consistent with the known result (see reference [19]).

6.2. ELASTIC FOUNDATION

If damping is ignored in equations (24) and (31), the viscoelastic foundation degrades to an elastic foundation and the FRFs become

$$\mathrm{H}_{Line}(\mathbf{x},\Omega) = \frac{1}{(2\pi)^2}\int_{-\infty}^{\infty}\int_{-\infty}^{\infty}\frac{\sin\xi r_0\exp(\mathrm{i}\boldsymbol{\xi}\mathbf{x})}{\xi r_0[D(\xi^2+\eta^2)^2+K-\rho h\Omega^2]}\,\mathrm{d}\xi\,\mathrm{d}\eta, \tag{34}$$

$$\mathrm{H}_{Con}(r,\Omega) = \frac{1}{2\pi}\int_0^{\infty}\frac{\mathrm{J}_0(r\zeta)}{D\zeta^4+K-\rho h\Omega^2}\,\zeta\,\mathrm{d}\zeta. \tag{35}$$

It is of interest to evaluate the integral of equation (34) for the displacement response of the center of the load. In this case, we have

$$\mathrm{H}_{Line}(0,\Omega) = \frac{1}{(2\pi)^2 r_0 D}\int_0^{2\pi}\int_0^{\infty}\frac{\sin(\zeta r_0\cos\psi)}{(\zeta^4+\bar{K}/D)\cos\psi}\,\mathrm{d}\zeta\,\mathrm{d}\psi, \tag{36}$$

where the equivalent stiffness $\bar{K} = K - \rho h\Omega^2$ and the transformations $\xi = \xi\cos\psi$ and $\eta = \zeta\sin\psi$ are used in the derivation of equation (36). We have the Taylor expansion

$$\frac{\sin(\zeta r_0\cos\psi)}{r_0\cos\psi} = \frac{1}{r_0\cos\psi}\sum_{n=0}^{\infty}(-1)^n\frac{(\zeta r_0\cos\psi)^{2n+1}}{(2n+1)!} = \sum_{n=0}^{\infty}(-1)^n\frac{r_0^{2n}\zeta^{2n+1}\cos^{2n}\psi}{(2n+1)!} \tag{37}$$

and the integration evaluated by parts

$$\int_0^{2\pi}\cos^{2n}\psi\,\mathrm{d}\psi = \left[\sin\psi\sum_{k=0}^{n-1}\frac{(2n)!(k!)^2\cos^{2k+1}\psi}{2^{2n-2k}(2k+1)!(n!)^2} + \frac{(2n)!\psi}{2^{2n}(n!)^2}\right]\Bigg|_0^{2\pi} = \frac{2\pi(2n)!}{2^{2n}(n!)^2}. \tag{38}$$

Substituting equations (37) and (38) into equation (36) we obtain

$$\mathrm{H}_{Line}(0,\Omega) = \frac{1}{4\pi D}\sum_{n=0}^{\infty}\frac{(-1)^n r_0^{2n}}{2^{2n}(n!)^2(2n+1)}\int_0^{\infty}\frac{u^{2n}}{u^2+\bar{K}/D}\,\mathrm{d}u, \tag{39}$$

where $u = \zeta^2$.

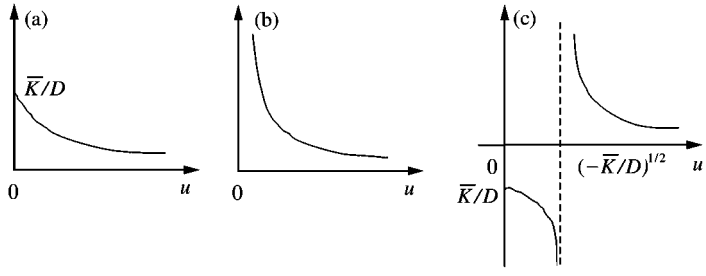

Figure 2. The curves of the integrand for different cases: (a) $\Omega < \Omega_0$, (b) $\Omega = \Omega_0$ and (c) $\Omega < \Omega_0$.

For the case of the excitation of a harmonic point load, $H_{Con}(0, \Omega)$ can be obtained by taking the limit on both sides of either equation (39) or equation (35). It is noted that $\lim_{z\to 0} J_0(z) = 1$ and we can further evaluate equation (35) for the limit as

$$H_{Con}(0, \Omega) = \lim_{r\to 0} \frac{1}{2\pi} \int_0^\infty \frac{J_0(r\zeta)}{D\zeta^4 + K - \rho h \Omega^2} \zeta \, d\zeta = \frac{1}{4\pi D} \int_0^\infty \frac{1}{u^2 + \bar{K}/D} \, du. \tag{40}$$

The integrand $(u^2 + \bar{K}/D)^{-1}$ is drawn in Figure 2 for the non-negative region of u. In the following, three distinct cases of the harmonic frequency Ω will be discussed for evaluating $H_{Con}(0, \Omega)$.

Equation (40) can also be written as

$$H_{Con}(0, \Omega) = \begin{cases} (4\pi\phi D)^{-1} \displaystyle\int_0^\infty (z^2 + 1)^{-1} \, dz, & \Omega < \Omega_0, \\ (4\pi D)^{-1} \displaystyle\int_0^\infty z^{-2} \, dz, & \Omega = \Omega_0, \\ (4\pi\phi D)^{-1} \displaystyle\int_0^\infty (z^2 - 1)^{-1} \, dz, & \Omega > \Omega_0, \end{cases} \tag{41}$$

where $\phi = (|\bar{K}|/D)^{1/2}$, and the resonance frequency $\Omega_0 = \sqrt{K/\rho h}$.

For the case $\Omega < \Omega_0$, it is straightforward to develop the integral of equation (41) into a closed form, i.e.,

$$H_{Con}(0, \Omega) = \frac{1}{4\pi\sqrt{\bar{K}D}} \operatorname{arctg} \sqrt{\frac{D}{\bar{K}}} u \Big|_0^\infty = A[1 - (\Omega/\Omega_0)^2]^{-1/2}, \tag{42}$$

in which $A = (8\sqrt{KD})^{-1}$. It can be seen that the amplitude of $H_{Con}(0, \Omega)$ tends to be infinite as the harmonic frequency approaches the resonance frequency.

For the case of $\Omega = \Omega_0$, since $\int_0^\infty z^{-2} \, dz = -z^{-1}|_0^\infty$, a singularity of the order $o(z^{-1})$ appears when evaluating an integral of this type. This means a resonance phenomenon will occur if $\Omega = \Omega_0$. Therefore, the integral of equation (41) becomes infinite and does not exist.

For the case of $\Omega > \Omega_0$, the complex function technique is used to evaluate this generalized integral. Two poles of the first order are found and they are, respectively, located at $(-1, 0i)$ and $(1, 0i)$ of the complex z-plane. Since integral (41) is integrated along the positive direction of the real axis, the pole at $(-1, 0i)$ does not contribute to the

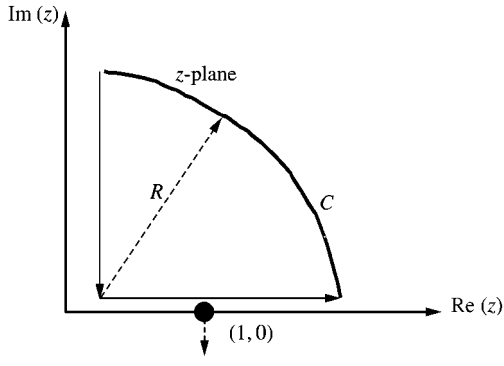

Figure 3. Integral contour for evaluating equation (41) in the case of $\Omega > \Omega_0$.

integration. As far as the other pole is concerned, it is exactly located on the positive real axis. However, if a small amount of damping is present, and this is always the case for any physical dynamic system in reality, this second pole will be slightly lower down into the fourth quadrant of the complex plane. Therefore, if an integral route is selected along the positive direction of the real axis, there is no need to construct a small contour, such as a half-circle with minus radius, to avoid encountering this pole.

The contour for evaluating this integral, plotted in Figure 3, consists of three segments, in which C represents a quarter-circle with a radius R. Clearly, no pole is embraced by this closed contour.

According to the theorem of residue, integration (41) along the closed route becomes zero as $R \to \infty$, i.e.,

$$\oint = \lim_{R\to\infty} \left(\text{p.v.} \int_0^R \int_C \int_R^0 \right) = 0, \tag{43}$$

in which the abbreviation, p.v., represents the Cauchy principal value of the integration $(4\pi\phi D)^{-1} \int_0^\infty (z^2 - 1)^{-1}\, \mathrm{d}z$. For the z value along the route $\int_R^0$, it is clear that we have $z = l\exp(\mathrm{i}\pi/2)$ and $\mathrm{d}z = \exp(\mathrm{i}\pi/2)\mathrm{d}l$. Hence, the integration

$$\lim_{R\to\infty} \left[(4\pi\phi D)^{-1} \int_R^0 (z^2 - 1)^{-1}\, \mathrm{d}z \right] = \lim_{R\to\infty} \left[-(4\pi\phi D)^{-1} \int_R^0 \mathrm{i}(l^2 + 1)^{-1}\, \mathrm{d}l \right]$$

$$= \mathrm{i}(4\pi\phi D)^{-1} \operatorname{arctg} l|_0^\infty = \mathrm{i}(8\phi D)^{-1}. \tag{44}$$

For the z value along the contour C_0, we have $z = \exp(\mathrm{i}\vartheta)R$ and $\mathrm{d}z = \mathrm{i}\exp(\mathrm{i}\vartheta)R\,\mathrm{d}\vartheta$ as $R \to +\infty$. The integration $\int_{C_2}$ becomes

$$\lim_{R\to\infty} \left[(4\pi\phi D)^{-1} \int_C (z^2 - 1)^{-1}\, \mathrm{d}z \right] = \lim_{R\to\infty} \left[(4\pi\phi D)^{-1} \int_0^{\pi/2} \frac{\mathrm{i}\exp(\mathrm{i}\vartheta)R}{1 - R^2\exp(\mathrm{i}2\vartheta)}\, \mathrm{d}\vartheta \right] = 0. \tag{45}$$

Comparing equations (43)–(45) and rearranging the order of the terms of formula (35), it is found that $\mathrm{H}_{Point}(0, \Omega)$ becomes

$$\mathrm{H}_{Con}(0, \Omega) = -\mathrm{i}A[\Omega/\Omega_0)^2 - 1]^{-1/2}. \tag{46}$$

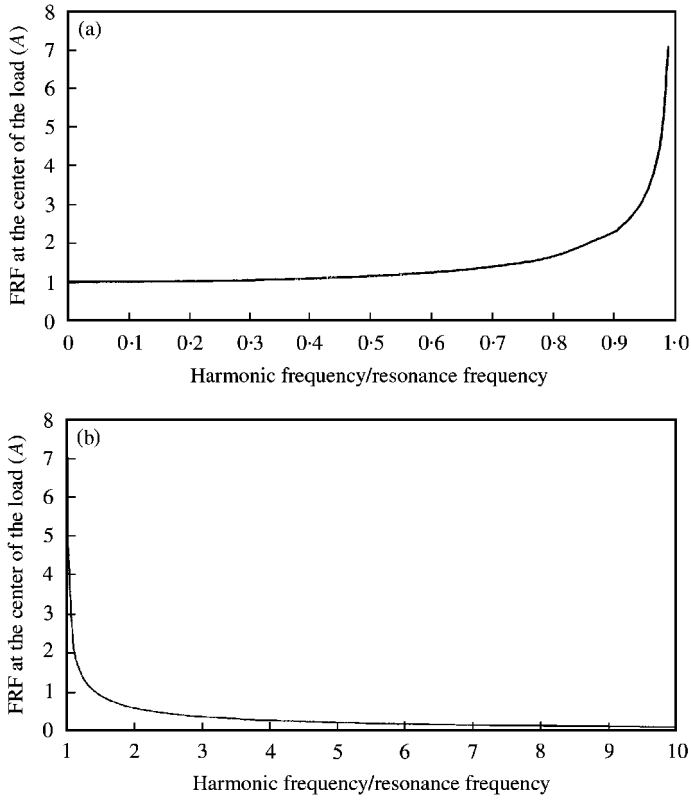

Figure 4. The FRF function $H_{Con}(0, \Omega)$ against the ratio of Ω/Ω_0: (a) $\Omega < \Omega_0$ and (b) $\Omega > \Omega_0$.

The amplitude of FRF at the location $(x, y) = (0, 0)$ with respect to the frequency Ω of the external load is shown in Figure 4. It can be seen that the amplitude of $H_{Con}(0, \Omega)$ tends to be infinite as the harmonic frequency approaches the resonance frequency.

7. CONCLUSIONS

The Fourier transform is used to derive the integral representation of the time–harmonic Green function of a plate under a line load. The dynamic deflection of a plate on a viscoelastic foundation subjected to both impulse and harmonic line loads are obtained by using the integral transformation method. The solution is first given as a convolution of the Green function of the plate. Poles of the integrand in the integral representation of the solution are identified for different cases of the foundation damping and the load frequency. The IRF is then obtained and can be numerically computed. A closed-form solution in terms of algebraic series corresponding to the FRF of the plate under a concentrated load is obtained. Numerical computation is used to illustrate the variation of FRF with respect to harmonic frequency. This analytical representation permits one to construct algorithms for the parameter identification of the inverse problem involved in pavement non-destructive test. The validity of the result is partly verified by comparing the static solution of a point source obtained from this paper to a well-known result.

ACKNOWLEDGMENTS

The author is grateful to the anonymous referees for their valuable comments, which enhanced the contents and presentation of this paper.

REFERENCES

1. A. J. BUSH 1980 *Final Report FAA RD*-80-9. Federal Aviation Administration. Nondestructive testing for light aircraft pavements, phase II. Development of the nondestructive evaluation methodology.
2. R. HASS, W. R. HUDSON and J. ZNIEWSKI 1994 *Modern Pavement Management*. Malabar, FL: Krieger Publishing Company.
3. O. S. SALAWU and C. WILLIAMS 1995 *Journal of Structural Engineering American Society of Civil Engineers* **121**, 161–173. Full-scale force–vibration test conducted before and after structural repairs on bridge.
4. J. UZAN and R. LYTTON 1990 *Journal of Transportation Engineering American Society of Civil Engineers*, **116**, 246–250. Analysis of pressure distribution under falling weight deflectometer loading.
5. H. M. S. WESTERGAARD 1926 *Public Roads* **7**, 90–112. Stresses in concrete pavements computed by theoretical analysis.
6. T. SCULLION, J. UZAN and M. PAREDES 1990 *Transport Research Rec*., No. 1260. MODULUS: a microcomputer-based backcalculation system.
7. A. R. KUKRETI, M. TAHERI and R. H. LEDESMA 1992 *Journal of Transportation Engineering American Society of Civil Engineers* **118**, 341–360. Dynamic analysis of rigid airport pavements with discontinuities.
8. M. R. TAHERI 1986 *Ph.D. Thesis*, *Purdue University*, *West Lafayette*, *IN*. Dynamic response of plates to moving loads.
9. S. M. ZAGHLOUL, T. D. WHITE, V. P. DRNEVICH and B. COREE 1994 *Transport Research Board*, *Washington*, *DC*. Dynamic analysis of FWD loading and pavement response using a three dimensional dynamic finite element program.
10. Z. DESHUN 1999 *Journal of Sound and Vibration* **221**, 187–203. A dynamic model for thick elastic plates.
11. J. BO 1999 *International Journal of Engineering Science* **37**, 379–393. The vertical vibration of an elastic circular plate on a fluid-saturated porous half space.
12. L. SUN and X. DENG 1998 *Journal of Transportation Engineering American Society of Civil Engineers* **124**, 470–478. Predicting vertical dynamic loads caused by vehicle–pavement interaction.
13. L. SUN 1998 *Final Report Prepared for National Science Foundation of China. Southeast University Nanjing. China*: Theoretical investigations on vehicle–ground dynamic interaction.
14. L. SUN and X. DENG 1997 *Chinese Journal of Applied Mechanics* **14**, 72–78. Transient response for infinite plate on Winkler foundation by a moving distributed load.
15. J. T. KENNEY 1954 *Journal of Applied Mechanics*, *American Society of Mechanical Engineers* **116**, 359–364. Steady-state vibrations of beam on elastic foundation for moving load.
16. E. J. YODER and M. W. WITCZAK 1975 *Principles of Pavement Design*. New York: John Wiley & Sons, Inc.
17. L. SUN and B. GREENBERG 2000 *Journal of Sound and Vibration* **229**, 957–972. Dynamic response of linear systems to moving stochastic sources.
18. G. N. WATSON 1966 *A Treatise on the Theory of Bessel Functions*. London: Cambridge University Press: second edition.
19. Z. ZHU, B. WANG and D. GUO 1984 *Pavement Mechanics*. Beijing, China: Renming Jiaotong Publishing Inc.